Modelling Thermal Time-of-Flight Sensor for Flow Velocity Measurement

O.Ecin*[1], E. Engelien[2], M. Malek[2], R. Viga[2], B. Hosticka[1], and A. Grabmaier[2]
University Duisburg-Essen, Department of Electrical Engineering and Information Technology,
[1]Institute of Microelectronic Systems, [2]Institute of Electronic Devices and Circuits
*Corresponding author: University Duisburg-Essen, Bismarckstr. 81, 47057 Duisburg, Okan.Ecin@uni-due.de

Abstract: This communication reports on a numeric fluid dynamics simulation on a pipe flow model. The basic background is to determine the velocity of a flowing fluid in a pipe by using the Thermal Time-of-Flight (TTOF) method on water. The visualisation of the temperature and velocity distribution in the pipe model is being carried out in order to enable proper design and optimisation of the TTOF sensor. The work is accomplished in two dimensional and three dimensional simulations. Transient simulations have been realised using the 2D simulation model. The flow velocity is calculated by means of the FFT-correlation technique. At several detection points the time-dependent temperarure signal is measured in a time period of ten seconds. The time delay of the output signals combined with the knowledge of the covered distances yields the flow velocity. In this work, a flow measurement technique in the velocity range $0.01\ \text{m/s} \leq v_m \leq 0.1\ \text{m/s}$ is presented for water.

Keywords: FFT-correlation, flow velocity, fluid flow, heat transfer, signal processing, Thermal Time-of-Flight (TTOF)

1. Introduction

The use of mass and volume flow measurement techniques is essential in the industry for process control purposes, e. g. of gases and liquids. In recent years several different types of sensors were developed. Depending on the standards, for example metering precision, flow ratio, permitted decrease of pressure and also for the cost of production, different measurement principles are applied. The utilization of these measurement systems is mostly dependent on pressure, temperature, density, viscosity and homogeneity of the fluid. Hence, flow sensors must be calibrated and maintained for certain application.

Thermal flow measurement is currently based on the measurement of displacement of heat against the velocity of the fluid (mass flow measurement). The heat pall is induced by a continuous heating element into the passing fluid. This kind of sensor is only applicable for homogeneous fluids with well known properties [1][3][5].

On the contrary, this presented investigation includes a discontinuous heating element offering a measurement technique to determine the flow of any kind of fluid with unknown properties (volume flow measurement). This basic approach is intended to be low-maintenance and exempt from calibration. The Thermal Time-of-Flight (TTOF) principle based on the induction of mobile heat pulses in the flow of gases and liquids is the key point of the investigations.

Heat as thermal energy is a quite suitable transfer marker for a wide spectrum of fluids – gases and liquids [4]. These are going to be investigated for water in its dynamics with the use of pipe flow models. In particular, determining the mean velocity of any fluid, for the Thermal Time-of-Flight method is applicable. The key point is to measure the time that the heat pulse propagates along a certain distance flowing through the pipe. Therefore, time discrete heat pulses are generated at a defined point in the pipe and are detected at minimum two defined sensing points. These points are located downstream. In addition, measuring flow velocity in both directions, more detection points have to be arranged upstream, respectively. Hereby, determining the flow direction is furthermore feasible.

The filament is biased with a specified signal sequence. Since a sequence of heat pulses is going to be injected into the fluid, a periodic pulse signal form is applied to the filament. The entire model can be regarded as a signal transmission process with a signal generator, transmission channel, and detection unit. The filament serves as the signal generator, the fluid itself acts as the transmission channel and finally thermal sensors form a detection unit.

2. Governing Equations

As a matter of fact, three basic equations are applied to the simulation of the TTOF sensor. These will be described in the following part considering fluid mechanics, heat transfer, and joule heating phenomena. In addition to the equations the transfer parameters will be described.

2.1 Fluid Mechanics

For simulating a liquid flow in a pipe Navier-Stokes equations from fluid mechanics are used. The fluid flow can be described by the conservation of momentum employing the Incompressible Navier-Stokes mode (chns) from the Chemical Engineering module of COMSOL multiphysics:

$$\rho\frac{\partial \boldsymbol{u}}{\partial t}+\rho\cdot\boldsymbol{u}\cdot\nabla\boldsymbol{u}-\boldsymbol{F} = \nabla\cdot\left[-p\mathbf{I}+\eta(\nabla\boldsymbol{u}+(\nabla\boldsymbol{u})^T)\right] \quad (1)$$

$$\nabla\boldsymbol{u}=0 \quad (2)$$

where $\boldsymbol{F}$ is a body force term [N·m^{-3}], ρ the density of the fluid [kg·m^{-3}], $\boldsymbol{u}$ the velocity [m·s^{-1}], η the dynamic viscosity of the fluid [N·s·m^{-2}] and p the pressure [N·m^{-2}]. In equation (1) the first two terms describe the inertia of the investigated volume, $\boldsymbol{F}$ external affected forces, $p{\cdot}\boldsymbol{I}$ the pressure at the volume in all directions and the last term the friction. Equation (2) gives the boundary condition by constant or nearly constant density ρ like in the case for all fluids.

2.2 Heat Transfer

The transport and dispersion of the generated heat result from a combination of forced convection and diffusion. The general heat transfer equation yields under consideration of heat conduction and heat convection [4]:

$$\rho\cdot c_p\frac{\partial T}{\partial t}+\nabla\cdot\left(-\lambda\nabla T\right) = Q-\rho\cdot c_p\cdot\boldsymbol{u}\cdot\nabla T \quad (3)$$

with T as the temperature [K], λ the specific thermal conductivity [W·m^{-1}·K^{-1}], c_p the specific heat capacity of the fluid at constant pressure [J·kg^{-1}·K^{-1}] and Q as the heat source [W·m^{-3}]. The equation (3) characterises the conservation of energy. Thereby is the first term the internal energy of a specified volume, the second for the thermal conduction, Q requires local heat sources and the last term stands for thermal convection (enthalpy flow). In COMSOL multiphysics the Convection and Conduction mode (chcc) from the Chemical Engineering module is adopted.

2.3 Joule Heating

The Conductive Media DC application mode (emdc) from the AC/DC module allows the effect of joule heating in a filament whereby electrical energy is converted to thermal energy. The equation (4) describes the reaction of voltage on the ends of a filament to a temperature on the surface. The equation is given by:

$$-\nabla\cdot(\sigma\nabla V-J^e)=Q_j \quad (4)$$

where σ is the electrical conductivity [m^{-1}·Ω^{-1}], V the electrical potential [V], J_e the externally generated current density [A·m^{-2}], and Q_j the current source [A·m^{-3}]. The conductivity is described in equation (5) as:

$$\sigma=\frac{1}{\rho_0(1+\alpha(T-T_0))} \quad (5)$$

with ρ_0 as electrical resistivity [m·Ω] at the reference temperature T_0 [K], and α as the temperature coefficient of resistivity [K^{-1}].

2.4 Material Parameters and Couple Factors

In the numeric simulation model water (ρ = 998 [kg·m^{-3}], λ = 0,598 [W·m^{-1}·K^{-1}], c_p = 4187 [J·kg^{-1}·K^{-1}] and η = 1,001 [mPa·s]) as flowing liquid and tungsten (ρ = 19250 [kg·m^{-3}], c_p = 130 [J·kg^{-1}·K^{-1}], κ = 18,38·10^6 [A·V^{-1}·m^{-1}], and α = 400 [W·m^{-1}·K^{-1}]) for the filament are applied. The values are given for a temperature T of 293.15 K. The material properties are taken out of the module library; thereby for temperature dependent parameters the functions are given.

For an interactive adjustment of the modes the transfer parameters must be initiated in other modes. On the one hand the parameter is the velocity ***u*** of the module chns of which the values are relevant for the chcc mode. On the other hand the temperature parameter T of the module emdc is needed first from the module chcc and the values of the heat distribution are given afterwards to the module chns to include the temperature T into the velocity flow field.

3. Numerical Model

Initially the 2D and 3D pipe flow models are described in the following section. The alignments of subdomain and boundary conditions applying to COMSOL multiphysics for the pipe flow models are explained afterwards.

3.1 Pipe Flow Models

For the investigations to determine flow velocity three pipe models (2D and 3D) have been created in Autodesk Inventor Professional 2010. The flow models have a length of $L = 0.1$ m and a diameter between the endwalls of $d_{Pipe} = 0.04$ m. A filament is placed 0.02 m behind the pipe entrance at a height of $y = 5.86$ mm and exhibits a square cross section of $H_{Fi} = 0.2$ mm * $L_{Fi} = 1$ mm. On the ends of the filament a voltage signal was applied to generate heat pulses. Heat detection is realised by arranging thermocouples (TCs) into the pipe downstream at the same distance, respectively.

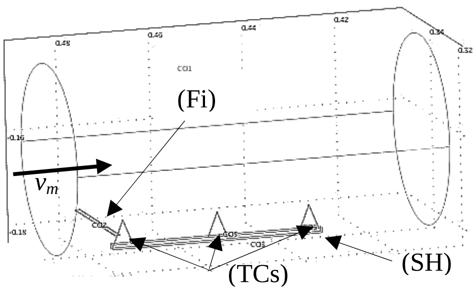

Figure 1: 3D pipe model of flow sensor construction with a filament (Fi) and a sensor holder (SH) including three thermocouples (TC).

The idea is to create increasingly simplified sensor construction models to facilitate the solving problem. Therefore, three models are created, each with less components in the heat flow line to understand on the one hand the influence of the thermocouples for the velocity distribution and on the other hand the variation of fluid flow and temperature distribution.

The first model (Figure 1) is adapted for our real experimental setup to verify the measured results. The pipe model has a filament with three thermocouples assembled on a holder in the line of the flowing heat pulses. The thermocouples are depicted in the figure as triangular geometry.

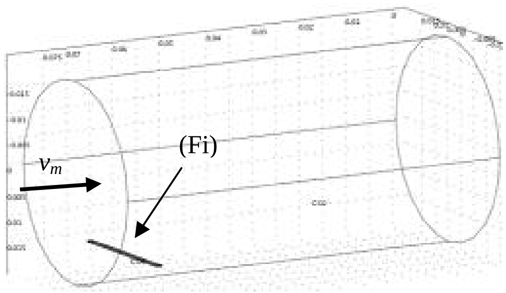

Figure 2: 3D pipe model with a filament (Fi).

The second model (Figure 2) is a simplification of the first one. The model consists of a pipe and the filament. This model is used for simplicity assuming the thermocouples have no relevant impact on the velocity distribution.

The third model (Figure 3) is a 2D representation of the second model. 2D models provide the best possibilities for a good simulation with less boundary condition.

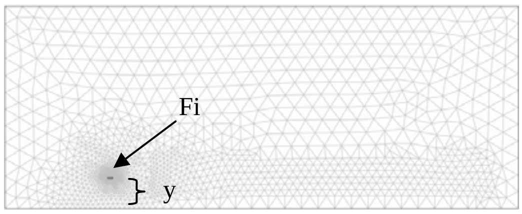

Figure 3: 2D mesh model for a liquid flow from left to right between two layers (at the top and on the bottom representing a pipe) with a filament (Fi) in the center of the fine meshed area (y is described in Figure 4).

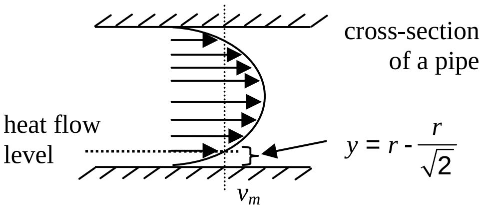

Figure 4: Parable of a laminar fluid flow with line of intersection for the mean velocity v_m and its crossing points (radius r = 20 mm).

In the experimental setup heat pulses are generated by a filament (Fi) located in the pipe (Figure 1 - Figure 3). For measuring the mean velocity v_m of the fluid at laminar flow the filament is positioned at a certain distance y = 5.86 mm relating to the radius of the pipe r = 20 mm (Figure 4).

Considering the critical Reynolds-Number of Re = 2300 for laminar flow range, the maximum flow velocity for water is approximately v = 0.05 m/s. This velocity was applied to the three models for comparison. The temperature of the flowing fluid is adjusted to T_{fluid} = 293.15 K. The temperature difference of the filament relating to the fluid is held in a maximum range of around $\Delta T \approx 10$ K.

3.2 Use of COMSOL Multiphysics

As has been noted, several physical phenomena are coupled for the simulation model. All phenomena are taken from the Chemical Engineering module as well as from the AC/DC module of the COMSOL application modes. For the 3D simulation the Incompressible Navier-Stokes mode (chns) resulting from momentum transport, the Convection and Conduction mode (chcc) resulting from energy transport, and also the Conductive Media DC mode (emdc) resulting from electro-thermal interaction are applied. Merely the last mode is neglected for the 2D simulation.

After the creation of the model drawing, the Incompressible Navier-Stokes mode is adopted first. Under the field physics the fluid type is chosen in the subdomain setting. Inlet and outlet conditions are defined in the boundary settings to laminar flow and to pressure with no viscous stress, respectively. The velocity value, inflow type, and entrance length of z_e = 1 m to form a laminar flow are modified at the inlet boundary. Remaining boundaries are set as wall types including the filament geometry and the pipe wall.

In the Convection and Conduction mode the fluid type has to be defined once again for the pipe geometry in the subdomain settings. Additionally, the velocity components u, v and w of the velocity field $\boldsymbol{u}$ have to be regarded. The initial temperature is set to T_0 = 293.15 K. In the boundary settings the initial temperature is appointed at the inlet boundary. The filament obtains a temperature rise of ΔT = 10 K relating to the initial value. At the outlet boundary convective flux is realised. The pipe wall boundaries are thermally insulated.

The filament material tungsten is selected in the Conductive Media DC mode in the subdomain settings under library material. Merely the filament geometry is active in this mode. In the boundary settings the ground side and the electrical potential side have to be conditioned, while the electrical potential signal has to be determined for generating dynamic thermal pulses.

Table 1 shows an overview of the modulation parameters at the different modes for the simulations' aim.

Table 1: Parameters settings at different modes.

Modes	Subdomain Settings	Boundary Settings
Incompr. Navier-Stokes	- library material: *fluid type*	- inlet: *velocity, entrance length*
Convection and Conduction	- library material: *fluid type* - velocity field: *(u v w)* - init value: *temperature*	- inlet: *temperature* - filament: *temperature* - outlet: *convective flux*
Conductive Media DC	- library material: *filament type* - init value: *electric potential*	- boundary condition: - *ground* - *electric insulation* - *electric potential*

4. Experimental Results

The 3D models are solved in the stationary domain. The transient calculations are accomplished for the 2D models.

In Figure 6 the stationary 3D model with the fluid water is depicted. The velocity distribution in the pipe for flowing water with a mean velocity of $v_m = 0.05$ m/s is simulated. Hereby, three thermocouples are involved in this simulation, which slightly influence the flow behaviour of the fluid. For this reason in the following simulations the downstream arranged thermocouples are for simplicity neglected.

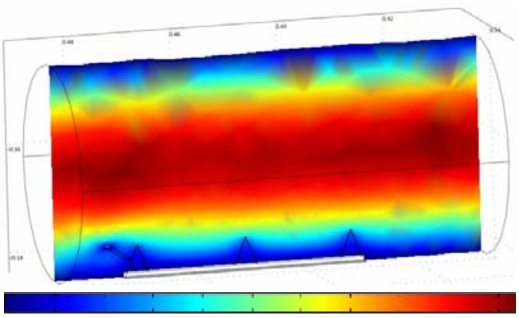

Figure 5: Stationary velocity distribution from 0 to 0.1 m/s (steps 0.01 m/s) of water with a mean velocity of 0.05 m/s for the 3D pipe model with filament and thermocouples.

Furthermore, it is more convenient to carry out the simulations without the use of the thermocouple structure. Figure 6 shows likewise a 3D model of water. Merely the filament influences the flow of the fluid.

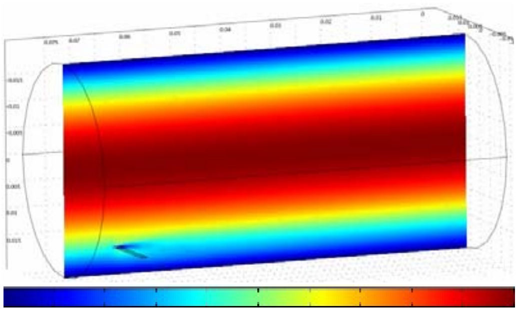

Figure 6: Stationary velocity distribution from 0 to 0.1 m/s (steps 0.01 m/s) of water with a mean velocity of $\boldsymbol{v_m} = 0.05$ m/s for the 3D pipe model with filament and thermocouples.

Since the flow behind the filament streams in its original homogenous state in a distance of $\Delta z = 3$ mm, the temperature signals can be measured downstream on the heat flow level of the filament to obtain the mean flow velocity.

Figure 7 illustrates the velocity distribution of flowing water in a 2D model with the filament as heat source. In multiphysics the mean velocity is adjusted to $v_m = 0.05$ m/s. The actual mean velocity on the 2D model is slightly varied. The influence of the filament on the flow in the 3D model as well as in the 2D model is quite similar, so that the 2D model is applied due to simplicity for the transient simulation. In both cases the change of the flow behaviour is less than 1 %. Acceleration is observed close to the filament due to the restriction of the cross section. This effect increases in the 2D model (Figure 5) compared to the 3D model (Figure 6).

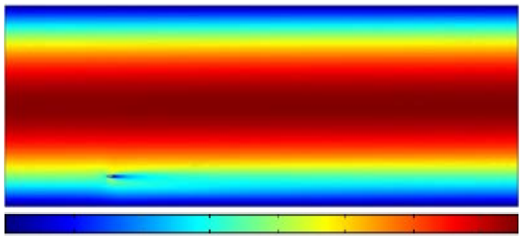

Figure 7: Stationary velocity distribution in the 2D model for laminar flow with a range from 0 to 0.075 m/s (steps 0.01 m/s).

In Figure 8 the temperature distribution is shown at the time when the heat pulse is activated at the filament. The temperature decreases exponentially in the subsequent 3 mm behind the filament to 2 % of the original generated temperature.

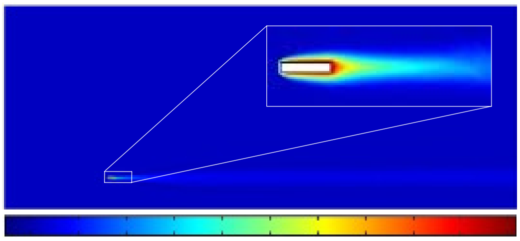

Figure 8: Stationary temperature distribution from 293 K to 303 K (steps 1 K) in the 2D model with a filament.

A temperature difference of $\Delta T = 0.2$ K downstream is still obtained. Hence, the temperature can be detected even in a distance that is sufficient for obtaining the original laminar flow.

The transient simulations applying on the 2D model are accomplished in a simulation time range of ten seconds. During this simulation time a short heat pulse with duration of $\Delta t_P = 0.5$ s is generated. The temperature signals are detected at five different points along the level of the filament in direction of the flow. The heat pulse strikes the first detection point $\Delta z = 0.02$ m behind the filament. The alongside detection points follow in flow direction each using the distance of $\Delta z = 0.01$ m. By means of Fast Fourier Transformation (FFT) the temperature signals are correlated to obtain the time shift between the detection points. The technique is known as FFT-correlation. Using signal processing methods the time delay of the temperature signals at several detection points can be calculated.

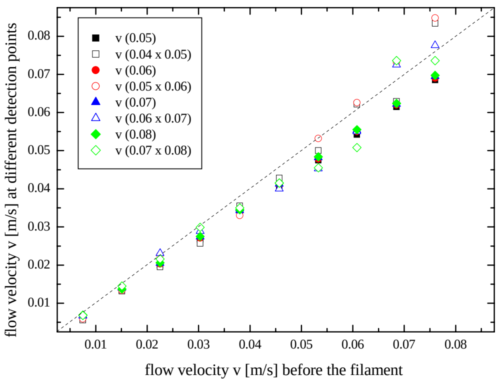

Figure 9: Comparison of the velocity on the heat flow level (Figure 4) before (abscissa) and behind the filament (ordinate).

Figure 9 shows a comparison of the actual mean flow velocity detected before the filament and at the detection points behind the filament as well as the calculated mean flow velocity. The detection points are located from $z = 0.04$ m to $z = 0.08$ m every 0.01 m. The detected temperature signal has been obtained using signal processing techniques. For obtaining the flow velocity at a certain detection point, the temperature signal of this detection point is correlated with the one from the previous detection point. Here, four velocities at $z = 0.05$ m, 0.06 m, 0.07 m and 0.08 m are presented.

The dashed line in Figure 9 characterises the ideal behaviour of the velocity before and behind the filament. All measurement points for each actual velocity are located very close to each other. For the velocities above $v = 0.05$ m/s, relating to the critical Reynolds-Number of $Re = 2300$, the measured velocities differ heavier from the ideal line. In particular, the actual velocities at the detection points show a great dependence on the actual velocity before the filament. A linear deviation of about 10 % of the actual velocities from the dashed line is observed. The FFT-correlated velocities show a higer deviation from the actual velocities above $v \geq 0.05$ m/s. A systematic deviation of the FFT-correlated velocities has not been observed.

5. Discussion

The assumed simplicities and approximations presented in the experimental results for neglecting the thermocouples are comprehensible. Regarding the geometries of the thermocouples and the associated meshing it is more convenient to solve such complex and coupled application modes in COMSOL multiphysics. In addition, the transient simulation implies further difficulties in solving the model.

In the simulations the behaviour of the flow velocity is recognisable in a good manner. The coupling of the temperature T and the velocity v is clearly presented in the 2D model (Figure 7 and Figure 8). The flow velocity is regained within the subsequent 3 mm behind the filament. A decay of the temperature of 2 % is observed. Considering the experimental setup thermocouples can be constituted for the detection of temperature changes of $\Delta T = 0.2$ K, whereas the temperature tail of the filament is small related to the detection area.

The demonstrated results in Figure 9 are calculated from the transient solved 2D model. This model is based on the previous, solved stationary model. The values for the actual velocities result from the stationary model. Obviously the calculated velocities from the transient simulation do not match with the actual velocities from the stationary simulation. This effect is based on the transient temperature signals.

6. Conclusions

In conclusion, a Thermal Time-of-Flight simulation has been demonstrated for the determination of flow velocity of fluids. Using heat as the transfer parameter is appropriate for Time-of-Flight measurements, since heat is applicable as transport phenomena in a wide spectrum of fluids. Furthermore, heat is an excellent marker in any fluid and can be induced in an extremely good way by heat conduction. Heat pulses propagating through a fluid are required for determining the time delay between the output signals. Hence, cross-correlation is the most suitable application method in the signal processing domain.

Going forward, different fluids - liquids and gases - are going to be investigated with this kind of measurement technique. Also gas mixture can be considered as inspecting medium. An important aspect is the analysis of the generated signal form to the results of the FFT-correlation. Referring to the input signal forms the so-called Pseudorandom Noise sequences (PN-sequences) can be taken into account for generating thermal pulses. These kinds of signal forms promise a more clearly pronounced cross-correlation peak, which is more adequate for higher flow velocities and even in the turbulent flow range of any fluid.

7. References

1. Ashauer, M. and Glosch, H.: “Thermal flow sensor for liquids and gases based on combinations of two principles”, Sensors and Actuators, pp. 7-13, 1999.

2. Bernhard, F.: “Technische Temperatur-messung: Physikalische und messtechnische Grundlagen, Sensoren und Messverfahren, Messfehler und Kalibrierung, Springer Verlag, ISBN 3540626727, 2004.

3. Bruschi, P. and Dei, M.: “Single chip sensing of multiple gas flows”, DTIP of MEMS & MOEMS, pp. 242-246, 2008.

4. Engelien, E., Ecin, O. et all: “Evaluation on Thermocouples for the Thermal Time-of-Flight Measurement”, 54th IWK, paper-id 87, pp. 1-5, Ilmenau, 2009.

5. Otakane, K. and Sakai, K.: “Development of the Thermal Flow Meter”, SICE Annual Conference, Vol. 3, pp. 3080-3083, 2003.

6. van Leyen, D.: “Wärmeübertragung: Grundlagen und Berechnungsbeispiele aus der Nachrichtentechnik”, Siemens AG, Berlin, 1971.

7. Webster, J. G.: “The Measurement, Instrumentation, and Sensors Handbook” CRC Press LLC, ISBN 3-540-64830-5, 1999.